DOSE DEPOSITION PROFILES IN UNTREATED BRICK MATERIAL

Ryan O'Mara and Robert Hayes*

Abstract—**In nuclear forensics or accident dosimetry, building materials such as bricks can be used to retrospectively determine radiation fields using thermoluminescence and/or optically stimulated luminescence. A major problem with brick material is that significant chemical processing is generally necessary to isolate the quartz from the brick. In this study, a simplified treatment process has been tested in an effort to lessen the processing burden for retrospective dosimetry studies. It was found that by using thermoluminescence responses, the dose deposition profile of a brick sample could be reconstructed without any chemical treatment. This method was tested by estimating the gamma-ray energies of an ^{241}Am source from the dose deposition in a brick. The results demonstrated the ability to retrospectively measure the source energy with an overall energy resolution of approximately 6 keV. This technique has the potential to greatly expedite dose reconstructions in the wake of nuclear accidents or for any related application where doses of interest are large compared to overall process system noise.**

Health Phys. 114(4):414–420; 2018

Key words: accident analysis; accidents, nuclear; dosimetry; dosimetry, thermoluminescent

INTRODUCTION

THE PHYSICAL mechanism of the thermoluminescence (TL) and optically stimulated luminescence (OSL) phenomena in insulators is based on the band model of solid state physics. In this model, the bonding electrons exist in the valence band, while the conduction band remains empty at room temperature. Defects in the crystal lattice lead to the formation of trap states that may exist in the energy gap between the valence and conduction bands. During exposure to ionizing radiation, electrons may be promoted from the valence band into the conduction band. In the presence of an electron in the conduction band, a trap state may capture an electron. The radiation dose absorbed by the material can be inferred by counting the number of trapped electrons. Generally speaking, trapped electrons will remain trapped until stimulated by an external energy source, thermal or optical, of sufficient energy to evict the electron from the trap. In this way, trapped electrons can create a permanent record of the dosimetric history of the sample.

It is assumed that the benefit to the nuclear forensics community of having a permanent record of radiation exposure is quite clear for security and attribution purposes to the extent that all historical sources can now be characterized. Luminescence dosimetry has been proposed for applications in both retrospective dosimetry and emergency dosimetry (Bailiff et al. 2016). In this context, the emergency dosimetry is distinct from retrospective dosimetry in that emergency dosimetry requires more rapid, reliable dose reconstructions. However, the applicability of luminescence methods is limited by a variety of factors, including long sample preparation times, the necessity of harsh chemical treatments for sample preparation, and that signal measurement is destructive to the signal. For both TL and OSL, it is beneficial to have samples that are optically transparent and very small in size, such as granular material. As a result, the sample preparation generally includes crushing the samples and treating them with harsh chemicals, such as HF and HCl, to remove any impurities from the material of interest along with the granular surface.

Very few studies have been conducted to determine whether a suitable signal can be acquired from samples that have not been chemically treated. However, Bøtter-Jensen et al. (1995) showed that radiation dose depth profiles could be directly measured with OSL scanning of untreated brick cores. Further studies have been conducted where dose deposition profiles have been measured in bricks from buildings located in areas heavily affected by nuclear fallout (Bailiff 1995; Bailiff et al. 2005; Ramzaev et al. 2008). In general, the results of such studies indicate that dose deposition profiles can be obtained using quartz extracted from clay bricks. One commonality between these studies is the necessity to isolate and extract quartz grains for the reconstruction of dose deposition profiles. The results presented below are the first in a series of studies that attempt to build

*North Carolina State University, Nuclear Engineering Department, Raleigh, NC.

The authors declare no conflicts of interest.

For correspondence contact: Ryan O'Mara, North Carolina State University, Nuclear Engineering Department, 1009 Capability Dr., Raleigh NC 27606 or emai at: **rpomara@ncsu.edu**.

(Manuscript accepted 15 *December* 2017)
0017-9078/18/0

DOI: 10.1097/HP.0000000000000843

on the work referred to above. One of the main goals of the work, presented herein, is to examine the ability of reconstructed dose deposition profiles to identify source material with minimal sample treatment.

The value in exploring such methods is twofold. First, one of the major disadvantages of luminescence techniques for retrospective dosimetry is that traditional sample preparation techniques can be time consuming, if not tedious (Bøtter-Jensen and Murray 2001). If satisfactory results can be obtained without the necessity of density separation and chemical treatment, then sample throughput should be able to be significantly increased. Second, negating the requirement of full wet chemistry laboratory procedures will represent a significant step toward the ability to make in-field dose measurements with luminescence analysis.

Another open-ended question with respect to luminescence dosimetry addressed in this work is how well bricks or other common building materials can discriminate differences in the energy of radiation sources. Assuming that the mineral composition and density of a sample material can be adequately known, it has been proposed that one way to estimate a source's energy would be to calculate the mass energy absorption coefficient μ_{en} of the material from the dose deposition profile in the material (Hayes and Sholom 2016). Under these assumptions, after the μ_{en} had been measured, it could be compared to the μ_{en} curve for the material from which the source energy could then be inferred. In neither the work presented here nor the work referenced above was the sensitivity of measured dose deposition profiles to brick composition specifically assessed. However, it is generally expected that, aside from the quartz content, uncertainties in the composition of the brick material are not a significant source of error in the measured dose deposition profiles.

There are number of factors that might limit the energy resolution from luminescence studies. One such limiting factor is how well the dose deposition profile in the material can be resolved. Therefore, the signal sensitivity of the measurement system will limit the energy resolving power of the technique. This paper demonstrates this concept by estimating the energy resolution of one retrospective dosimetry system from experimental data collected from an irradiated brick sample.

MATERIALS AND METHODS

A. Dose deposition profile measurement

Generic red bricks were purchased at a local supply store for this work. A 3.7 GBq encapsulated ^{241}Am source was placed between two bricks for 3 h 18 min. Four Landauer (Glenwood, IL, USA) nano-Dot optically stimulated luminescence dosimeters (OSLDs) were placed around the source to help assess the ability of the method to reconstruct the historical source location and provide an independent measure of the dose. Fig. 1 shows the exposure configuration with the top brick removed. The encapsulated ^{241}Am source was laid on top of the bottom brick, and then the second brick was placed on top of the first brick, sandwiching the source and the OSLDs.

A Monte Carlo n-particle (MCNP) model of the exposure configuration was then built from the photographs made during irradiation. The simulated brick was initially assumed to have a standard chemical composition and density (McConn et al. 2011). The results of the MCNP simulations were compared to the measured doses to the OSLDs. The relative difference between the measured and simulated OSLD doses were then used to update the source position. In this way, the position of the source was iteratively determined from the measured values of the doses to the OSLDs. The source position determined from the MCNP simulations was then verified using measurements from the photographs taken during the irradiation of the bricks.

The MCNP *pstudy* module (Brown et al. 2004) was then used to perform a perturbation analysis on the exposure simulation to holistically obtain complete uncertainty estimations. In the *pstudy* analysis, each nominal parameter in the simulation was independently perturbed around the measured or assumed value. For example, the brick composition, core location and angle, source location, OSLD location, and brick dimensions were all included in the perturbation analysis. A total of 400 test cases were run in an attempt to fully characterize the uncertainty distribution to the OSLDs and core layers. Fig. 2 shows a lateral projection from the simulated exposure configuration base case. By comparing the results of the MCNP simulations to the doses measured to the OSLDs, the location and activity of the source relative to the locations of the OSLDs was independently verified. As chemical compositions of the brick were not independently obtained, these were allowed to vary in the *pstudy* analysis by as much as 20% of their nominal values (so a 10 weight percent element would vary between 8 and 12%).

After localizing the source position, a 1-inch-diameter core was taken perpendicular to the irradiated surface of the

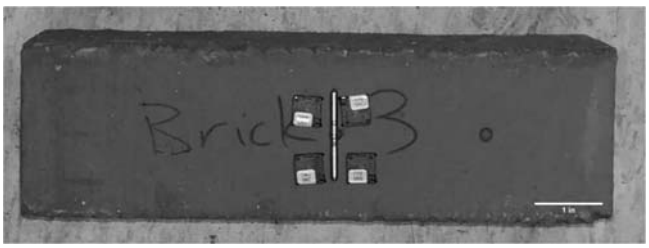

Fig. 1. Experimental exposure configuration. The source, centered metal rod, was placed on the brick between 4 nano-Dot OSLDs. The OSLDs served as independent verification of the exposure to the brick sample.

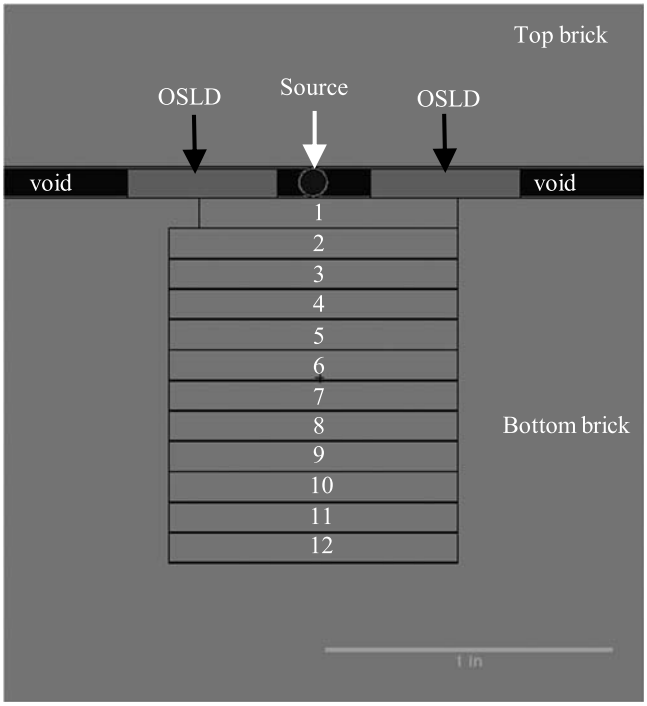

Fig. 2. Example of the exposure configuration model constructed in MCNP. The source (white arrow) is shown perpendicular to its axis on top of the core with its horizontal slices (numbered 1 through 12). The saw blade kerfs were included in the simulation, but are not evident in the image due to their small width. Two of the nano-Dot OSLDs (black arrows) are shown as well.

brick, from directly under the experimentally determined source location. During the drilling of the core, chatter in the drill bit damaged the top layer of the sample, as reflected in Fig. 2. The damage resulted in the loss of material from one side of the top layer, reflected by the smaller diameter of the top core layer (numbered 1) in Fig. 2. The removed core was then soaked overnight to ensure that the brick matrix was saturated. After soaking, the volume of the core was measured using liquid displacement. Following the volume measurement, the core was then oven-dried at 40°C for 3 d, and the mass was measured. The density of the core was then determined to be 2.24 g cc^{-1}. The measured core density was used to update the original MCNP model for subsequent calculation of the theoretical dose to each layer of the sample core.

The brick core was then sliced perpendicular to its axis into twelve approximately 2-mm-thick wafers using a low-speed, water-cooled Buehler IsoMet saw. All cuts were made using a diamond-grit cutting disk operated at 200 revolutions per minute (rpm). The placement of the cuts for each wafer were determined using the saw's built-in material feed indicator. Based on the MCNP calculations, the dose to the brick at depth of 3 cm was expected to be approximately 30 mGy, close to the detection limit expected. Since this study used the luminescence signals from polymineral brick samples, only 12 slices were taken from the core because it was assumed that the detection limit for the luminescence signals would be higher than 30 mGy. The 12 slices were then crushed and sieved into two grain size ranges, 90 to 250 μm and less than 90 μm. The 90 to 250 μm were saved for further processing and later comparison; i.e., density separation and/or chemical treatment (Colarossi et al. 2015).

To test the abilities of OSL to measure dose depth profiles with minimal processing, grains <90 μm were used. With no further processing, TL/OSL measurements were made on the <90 μm grains using a Risø TL/OSL-DA-20 reader (DTU Nutech, Kgs. Lyngby, Denmark) fitted with blue light-emitting diodes for OSL stimulation. The measurement approach was a modified version of the single aliquot regenerated dose (SAR; Wintle and Murray 2006) protocol using pulsed infrared stimulated luminescence (PIRSL) (Colarossi et al. 2015). Table 1 shows the specific steps used here.

Fig. 3 shows an example of the TL and IRSL curves obtained for slice 1 (closest to the source) and slice 6. In slice 6, it was found that the IRSL signal was comparable to the noise level in the authors' instrument and was therefore of limited utility. As was expected, the detection limit for the OSL signal in untreated brick samples was greater than would be expected for a pure quartz sample. However, the TL signal for these samples exhibited a much better signal-to-noise ratio than that of the OSL in the sequence and was therefore selected to reconstruct the dose. Subsequently, the signal of interest was taken to be the TL signal obtained during step two from Table 1. As a result, the SAR protocol was applied using these TL signal portions to determine the natural and regenerated doses, as opposed to the more traditional IRSL signal.

Referring to Table 1, the modified-SAR protocol used to reconstruct the dose deposition profiles began with a 260 °C isothermal TL glow curve collected by heating the

Table 1. Outline of the single aliquot protocol used for TL and OSL dose measurements.

Step	Description
Step 1	Dose (β source exposure, 0s for natural dose)
Step 2	"Preheat" (TL at 260 °C for 10 s)[†]
Step 3	Infrared stimulated luminescence (40 s at 220 °C)
Step 4	Pulsed optically stimulated luminescence (250μs total, 50 μs on, 50 μs off)
Step 5	Test dose (β source exposure for 300 s)
Step 6	"Preheat" (TL at 260 °C for 10s)
Step 7	Infrared stimulated luminescence (40 s at 220 °C)
Step 8	Pulsed optically stimulated luminescence (250 μs, 50 μs on, 50 μs off)

[†]Signal component used for final dose reconstruction.

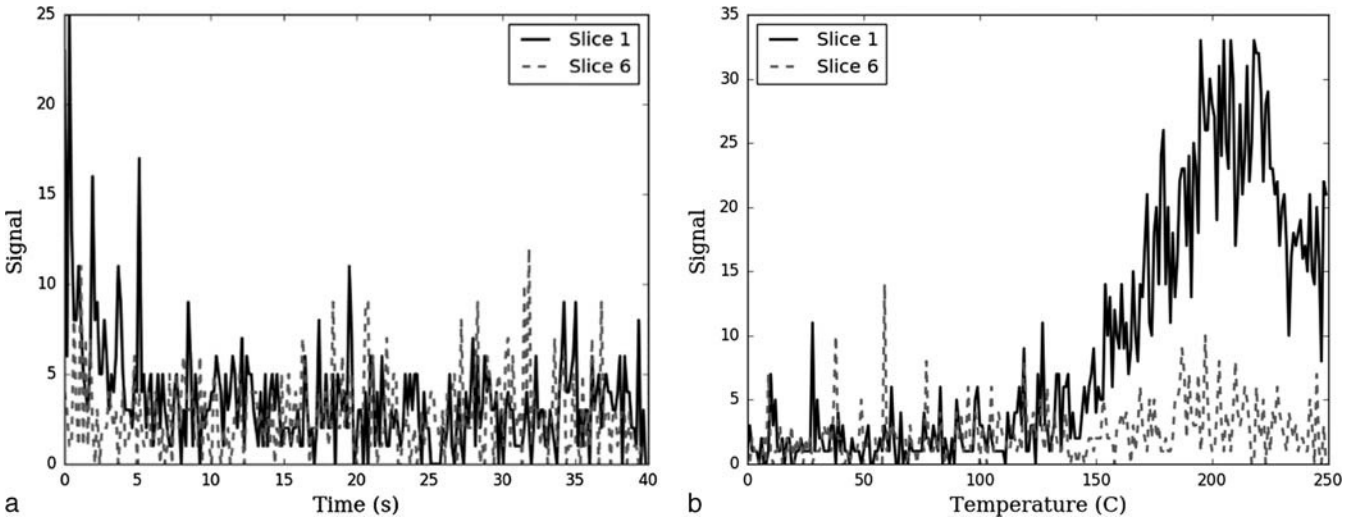

Fig. 3. IRSL/TL curves for slice 1 (solid) and slice 6 (dashed). The respective plots show the comparison between the magnitudes of the curves for the two slices. Since the dose is estimated from the area under the curve, the larger the vertical displacement of the curve, the higher the estimated dose. Here, the left image (a) shows the IRSL signal from slices 1 and 6 with the right image (b) showing TL from slices 1 and 6.

sample at 5 °C s^{-1} and holding it at 260 °C for 10 s. Next an OSL read (not used) was performed using infrared LEDs at 220 °C. Following the initial OSL read, a pulse OSL (not used) read was performed using blue LEDs. However, a software malfunction was experienced in which the time-of-arrival for the pulsed OSL data were not saved, preventing the use of the pulsed OSL data in the dose reconstruction. A test dose of 300 s was then applied, and a 260 °C TL glow curve was obtained using the same heating rate. Finally, the OSL and pulsed OSL steps were repeated (not used) using the infrared LEDs.

Because the source was placed directly on the surface of the brick, the assumption of a plane wave source could not be applied. As a result, the theoretical dose deposition was calculated by MCNP. The gamma distribution for the simulations was simplified to include only three of the main photons (59.5 keV, 13.9 keV, and 26.4 keV) emitted by ^{241}Am. The parameter study (*pstudy*), discussed above, was used to quantify the total uncertainty in the simulated dose values to each slice from the core. Comparison of the simulated dose deposition profile to the measured dose deposition profile was used to qualitatively assess the agreement between theory and measurement.

B. Source energy and energy resolution estimation

A relative profile matching technique was used to estimate energy resolution potential from the measured dose deposition profile. By this method, candidate dose deposition profiles were evaluated on the basis of the "goodness of fit" with measured dose deposition profiles. The merit function for assessing the "goodness of fit" was taken to be the sum of the squared residuals between the measured and simulated doses to each layer.

MCNP simulations were run to calculate the dose deposition profiles for 11 perturbed energies around the mean of the three main photon energies (59.5 keV, 13.9 keV, and 26.4 keV) in the ^{241}Am gamma spectrum. The energy of each photon was offset either positively or negatively by one-third of total energy perturbation for each step, but in all cases, each photon energy was perturbed in the same direction. The largest total negative perturbation was 3 keV (each photon energy was decreased by 1 keV), while the largest positive perturbation was 8.0 keV. It was assumed that the dose rate of the source was known from the measured doses to the OSLDs. From this, the sum of the squared residuals for the dose to each sample layer between each of the simulated cases and the measurements were calculated. The optimal source energy was determined to be the energy that minimized the sum of the squared errors between model and measurement.

The sums of the squared errors were plotted as a function of the perturbed source energies. For some small range of energy, this distribution will be reasonably approximated by a quadratic function. Within this small range, the shape can be approximated by an inverted Gaussian. This approximation assumes that the deviation of the true attenuation profile from those obtained at offset energies will be normally distributed over some small range near the optimum energy. The distribution of the squared residuals in this range was inverted and considered to be approximately Gaussian. The shape parameter (root of the variance or standard deviation) of the distribution then gives a measure of the spread of the energies around the best-fit energy, or the energy resolution estimate. The inverted distribution of squared residuals was then fit with a Gaussian function. The mean of the Gaussian fit function was compared to

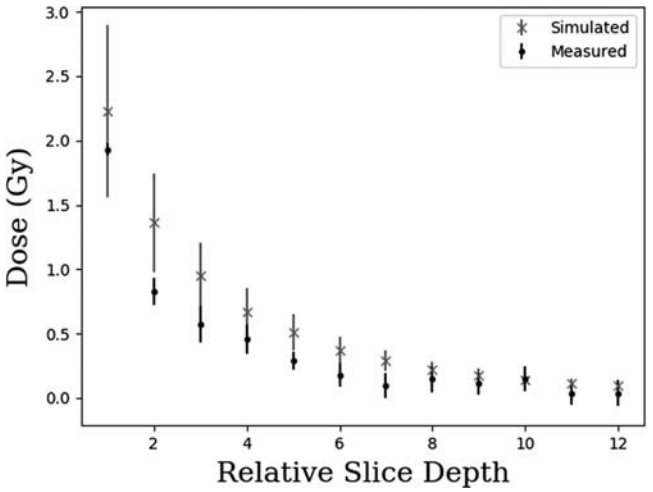

Fig. 4. Plot of the measured (black dots) and simulated (grey X's) dose for each of the twelve brick slices. In this figure, the abscissa represents the relative position of the slice with respect to the source.

the measured source energy. The standard deviation of the Gaussian fit was taken to be the energy resolution metric of the method as described above.

RESULTS AND DISCUSSION

A. Source energy determination

Fig. 4 shows the measured doses (black dots) to each of the twelve slices plotted with the MCNP simulated values (grey X's) for the doses to the corresponding layer. The error bars on the simulated values are the total 1σ uncertainty in the simulated values obtained from the MCNP *pstudy* parameter study. It can be seen that the simulated values for the doses are consistently larger than the measured doses. Previous studies measuring dose deposition in bricks have observed similar offset between measured and simulated values and have attributed the offset, at least in part, to instrument calibration (Hayes and Sholom 2016). The calibration of the source in the OSL/TL reader is material specific, and if the sensitivity or dose response of the sample material is significantly different from the calibration material, then over- or underestimation of reconstructed doses can be expected. The calculated values from MCNP were based on the Landauer OSLD measurements, and the brick doses were based on the TL/OSL reader calibration using Risø calibrated quartz (Hansen et al. 2015). As a result, some bias can reasonably be attributed to this source of uncertainty but not quantified from this work. Calibration comparisons are underway and planned for future work.

Another source of uncertainty in this experiment is the simplifying assumption that the ^{241}Am gamma spectrum was composed of only three gamma energies. Several other low energy gamma rays are also present in the emission spectrum of ^{241}Am but with branching ratios more than an order below those modeled here. However, the 59.5 keV gamma ray heavily dominates the emission spectrum, and it is expected that gamma rays with lower energies would only contribute to the dose in the top layers of the core although already attenuated from the encapsulation source.

Simple challenges with this technique for retrospective characterization of nuclear material include the unknown spatial and energy distributions along with the activity and dwell time of the source. Uncertainties in entrance dose can in many instances be assumed to be comparable, if not small, with respect to the uncertainty in the product of source activity and exposure time, so these are nominal issues. It is expected that if no information is known about the source isotopics, then single decay curve fit estimates of the source energy should tend toward the weighted mean of the energies in the source's gamma spectrum. A confounding effect can occur in spatial configurations where an assumption of simple exponential attenuation is not valid due to the incident radiation field not being a plane wave. Notably, the plane wave assumption is violated when the source is close to the layers being measured. This effect was mitigated here by taking credit for the known source distribution and only focusing on the question of accuracy and precision in energy discrimination. In general, a gridded sampling array would be needed to account for this method's ability to reconstruct a source's location. The location, once identified, can then be accounted for (as done here) when evaluating its effect in the dose deposition profile when material attenuation is used to estimate the incident gamma spectrum.

Fig. 5 shows the square of the residuals plotted vs. the perturbed simulated source energies. As expected, there is an approximately quadratic functional behavior. Referring to Fig. 5, it can be seen that the minimum in the sum of the squared residuals corresponds to a total positive energy offset of 2 keV. For the three photon energies in the

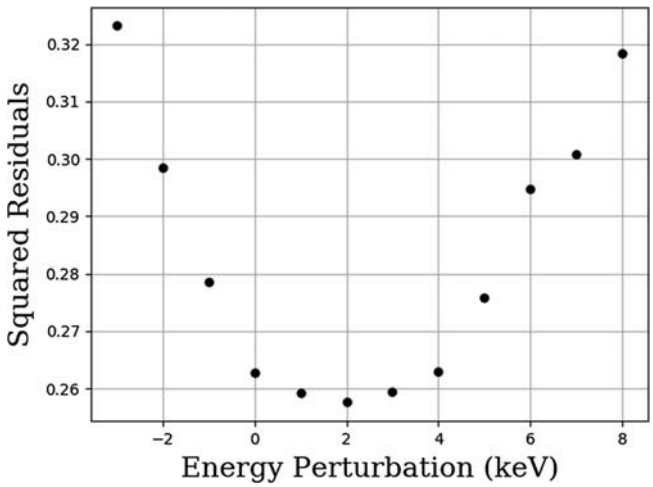

Fig. 5. Sum of the squared residuals for exponential fits to the measured dose deposition profile.

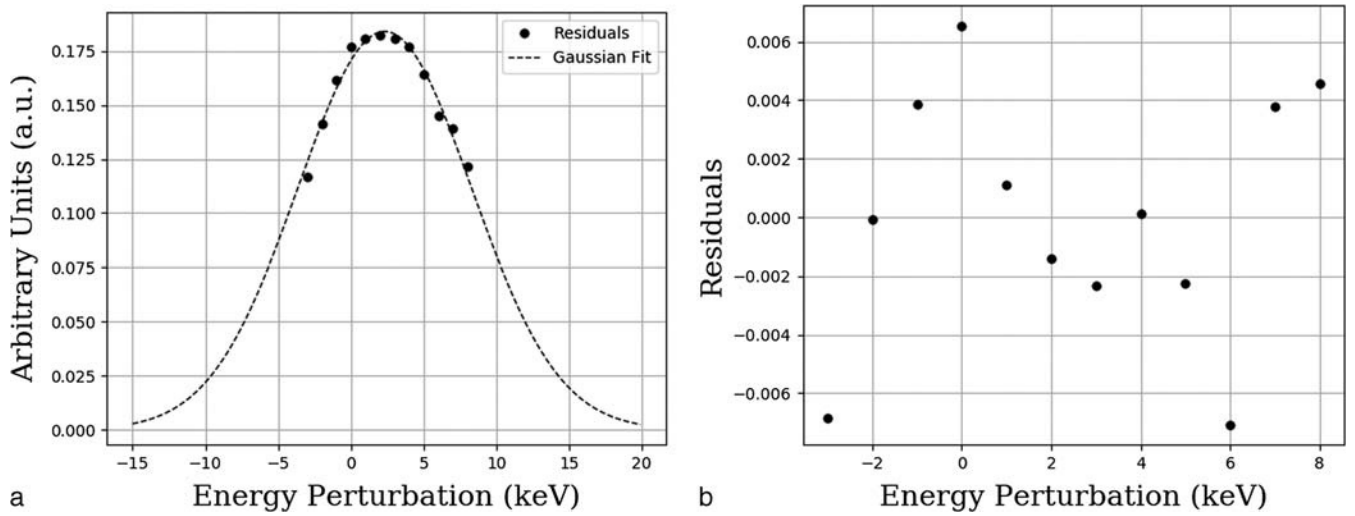

Fig. 6. (a) Plot of the Gaussian fit to the inverted residuals obtained by perturbing the source energy for the simulated dose deposition profile difference with the measured values; (b) Plot of the residuals for the Gaussian fit to the inverted squared residuals.

simulation, this corresponds to optimum energies 60.17 keV, 27.07 keV, and 14.57 keV.

B. Energy resolution estimation

Fig. 6a shows the inverted squared residuals, along with the Gaussian fit from the perturbed energy dose deposition simulations being fit to the measured data. Fig. 6b shows the fit residuals from the Gaussian approximation to the data. The best fit for the Gaussian was based on a chi-squared minimization. The Gaussian fit estimated the mean of the residual data to be 2.3± 0.2 as an accuracy metric in this instance. As expected, the "average" of the Gaussian coincides with the minimum of the simulation source energy residuals. Fig. 6b shows the residuals from the Gaussian fit.

The estimated standard deviation of the Gaussian fit was calculated to be 5.967±0.002, corresponding to an energy resolution of approximately 6 keV. It should be noted that the energy resolution is also a function of the mass energy absorption coefficient of the irradiated material, which is highly energy dependent. As a result, the energy resolution determined here is somewhat specific to the exposure conditions considered.

The energy resolution calculated here is promising for forensics applications. With energy resolutions on the order of 10%, development of algorithms to fit simulated dose deposition profiles to measured dose deposition profiles may allow for crude, retrospective isotopic analysis of source material. This advance may even allow for spent fuel characterization using luminescence and/or electron paramagnetic studies. It has been shown in previous work that spent fuel has a unique gamma spectrum characteristic of its initial enrichment and burnup and cool down time (Favalli et al. 2016). As a result, dose deposition profiles in materials exposed to the gamma field of spent fuel will have a unique shape. Using the methods presented here, it may be possible to perform dose deposition profile matching to estimate the burnup or initial enrichment of spent nuclear fuel from materials at the periphery of the spent fuel pool, even when that fuel is not available for direct measurement.

Gradient-based nonlinear optimization routines, such as the Levenberg-Marquardt (LM) method, have been shown here to be useful in determining the source energy distribution. The LM method is a nonlinear least squares method that combines the steepest descent approach and the Gauss-Newton method (Press et al. 2002). A full explanation of the LM method is beyond the scope of this analysis, but suffice it to say that the LM method uses gradients of a functional to minimize the chi-squared and thereby optimize the parameters of the functional. For this case, an LM

Table 2. Comparison of measured and simulated slice doses.

Slice Number	Measured dose (Gy)	Simulated dose (Gy)	Percent difference
Slice 1	1.93±0.04	2.2±0.7	−15.3
Slice 2	0.8±0.1	1.4±0.0.4	−64.3
Slice 3	0.6±0.1	0.9±0.3	−66.9
Slice 4	0.5±0.1	0.7±0.2	−46.4
Slice 5	0.29±0.07	0.5±0.1	−70.6
Slice 6	0.18±0.09	0.4±0.1	−108.4
Slice 7	0.10±0.09	0.29±0.08	−190.8
Slice 8	0.15±0.09	0.22±0.06	−57.8
Slice 9	0.11±0.08	0.18±0.05	−63.1
Slice 10	0.15±0.09	0.14±0.04	4.74
Slice 11	0.04±0.09	0.12±0.03	−207.5
Slice 12	0.04±0.1	0.10±0.03	163.3

routine would need to calculate the gradients for the dose to each sample layer with respect to the source energy. Calculation of the first order derivatives of the dose to each sample layer with respect to photon energy will be the primary hurdle to the implementation of a relative profile-matching scheme if it is not based on library profiles for sources with multiple photon energies (which could address this liability outright). Preliminary investigation suggests that finite differencing may be able to provide sufficient estimates of the needed gradients. However, approximating the derivatives with a finite difference would significantly increase the number of forward MCNP calculations needed to obtain a candidate dose deposition profile.

CONCLUSION

It has been demonstrated that dose deposition profiles can be obtained from minimally prepared brick samples of small grain sizes using TL in a SAR protocol and that these dose deposition profiles can be used to estimate the source energy distribution. Although there was some disagreement between the simulated and measured doses, the bias in source energy estimated from the dose deposition profile was within 3% of the known source energy. This is an important development with respect to rapid processing of samples in the wake of nuclear events where high throughput may be more important than precision or small detection limits. It should be noted, though, that these results are dependent on the mass energy absorption coefficient (μ_{en}) of the photon energies in the gamma spectrum of the source. At high gamma energies, the μ_{en} curve begins to flatten out. As a result, the ability to resolve closely spaced gamma ray energies would be reduced if source library distributions are not used. Additionally, potential calibration issues were identified and warrant future attention. The bias in the dose deposition profile introduced by these calibration issues could be the primary source of disagreement between the measured and known gamma ray energy distribution. Finally, it was estimated that the method's energy resolution for 241Am is approximately 10%.

Disclaimer—This report was prepared as an account of work sponsored by an agency of the United States Government. Neither the United States Government nor any agency thereof, nor any of their employees, makes any warranty, express or implied, or assumes any legal liability or responsibility for the accuracy, completeness, or usefulness of any information, apparatus, product, or process disclosed, or represents that its use would not infringe privately owned rights. Reference herein to any specific commercial product, process, or service by trade name, trademark, manufacturer, or otherwise does not necessarily constitute or imply its endorsement, recommendation, or favoring by the United States Government or any agency thereof. The views and opinions of authors expressed herein do not necessarily state or reflect those of the United States Government or any agency thereof.

Acknowledgments—This material is based upon work supported by the Department of Energy National Nuclear Security Administration under Award Number(s) DE-NA0002576. This work partially paid for by the Nuclear Regulatory Commission grant NRC-HQ-84-14-G-0059. Additional support of this work was through a joint faculty appointment between North Carolina State University and Oak Ridge National Laboratory in coordination with the Office of Defense Nuclear Nonproliferation R&D of the National Nuclear Security Administration sponsored Consortium for Nonproliferation Enabling Capabilities (CNEC). The authors declare no conflict of interest.

Authors' Note—After submission of this manuscript, a light leak was discovered during radioluminescence experiments. The effect of the light leak has not been quantified but may partially explain the negative bias observed in the measured data. Subsequent characterization of the effect is ongoing.

REFERENCES

Bailiff IK. The use of ceramics in retrospective dosimetry in the Chernobyl exclusion zone. Rad Meas 24:507–511; 1995.

Bailiff IK, Stepanenko VF, Goksu HY, Bøtter-Jensen L, Correcher V, Delgado A, Jungner H, Khamidova LG, Kolizshenkov TV, Meckbach R, Petin DV, Orlov MYu, Petrov SA. Retrospective luminescence retrospective dosimetry: development of approaches to application in populated areas downwind of the Chernobyl NPP. Health Phys. 89:233–246; 2005.

Bailiff IK, Sholom S, McKeever SWS. Retrospective and emergency dosimetry in response to radiological incidents and nuclear mass-casualty events: a review. Rad Meas 94:83–139; 2016.

Bøtter-Jensen L, Junger H, Poolton NRJ. A continuous OSL scanning method for analysis of radiation depth-dose profiles in bricks. Rad Meas 4:525–529; 1995.

Bøtter-Jensen L, Murray AS. Optically stimulated luminescence techniques in retrospective dosimetry. Radiat Phys Chem 61: 181–190; 2001.

Brown FB, Sweezy JE, Hayes RB. Monte Carlo parameter studies and uncertainty analyses with MCNP5. PHYSOR 2004 the physics of fuel cycles and advanced nuclear systems: global developments. LaGrange Park, IL: American Nuclear Society; 2004.

Colarossi D, Duller GAT, Roberts HM, Tooth S, Lyons R. Comparison of paired quartz OSL and feldspar post-IR IRSL dose distributions in poorly bleached fluvial sediments from South Africa. Quaternary Geochronol 30:233–238; 2015.

Favalli A, Vo D, Grogan B, Jansson P, Lijenfeldt H, Mozin V, Schwalbach P, Sjöland A, Tobin SJ, Trellue H, Vaccaro S. Determining initial enrichment, burnup, and cooling time of pressurized-water-reactor spent fuel assemblies by analyzing passive gamma spectra measured at the Clab interim-fuel storage facility in Sweden. Nucl Instr Meth Phys Res A 820: 102–111; 2016.

Hansen V, Murray A, Buylaert JP, Yeo EY, Thomsen K. A new irradiated quartz for beta source calibration. Rad Meas 81: 123–127; 2015.

Hayes RB, Sholom SV. Retrospective imaging and characterization of nuclear material. Health Phys 113:91–101; 2017.

McConn RJ Jr, Gesh CJ, Pagh RT, Rucker RA, Williams RG III. Compendium of material composition data for radiation transport modeling. Richland, WA: Pacific Northwest National Laboratory; PIET-43741-TM-963, PNNL-15870 Rev. 1; 2011.

Press WH, Teukolsky SA, Vetterling WT, Flannery BP. Numerical recipes in C: the art of scientific computing (reprinted with corrections). Cambridge: Cambridge University Press; 2002.

Ramzaev V, Bøtter-Jensen L, Thomsen KJ, Andersson KG, Murray AS. An assessment of cumulative external doses from Chernobyl fallout for a forested area in Russia using optically stimulated luminescence from quartz inclusions in bricks. J Environ Radioact 99:1154–1164; 2008.

Wintle AG, Murray AS. A review of quartz optically stimulated luminescence characteristics and heir relevance in single aliquot regeneration dating protocols. Radiat Meas 41: 369–391; 2006.